

# SPIN EFFECTS IN THE $\tau$ -LEPTON PAIR INDUCED BY ANOMALOUS MAGNETIC AND ELECTRIC DIPOLE MOMENTS\*

A.YU. KORCHIN 

NSC Kharkiv Institute of Physics and Technology, 61108 Kharkiv, Ukraine  
and

V.N. Karazin Kharkiv National University, 61022 Kharkiv, Ukraine  
and

M. Smoluchowski Institute of Physics, Jagiellonian University  
30-348 Kraków, Poland

*Received 5 February 2026, accepted 10 February 2026,  
published online 22 April 2026*

The possible anomalous New Physics contributions to magnetic and electric dipole moments of the  $\tau$  lepton have brought renewed interest in studying  $\tau$  pair production at energies of the LHC and future colliders. We discuss effects of electromagnetic and weak dipole moment contributions to the  $\tau$ -lepton polarization and  $\tau\tau$  spin correlations in the  $\gamma\gamma \rightarrow \tau^-\tau^+$  and  $q\bar{q} \rightarrow \tau^-\tau^+$  processes. Such processes have been observed in the  $pp$  and PbPb collisions in the LHC experiments. Extensions of the Standard Model amplitudes for  $\gamma\gamma \rightarrow \tau^-\tau^+$  and  $q\bar{q} \rightarrow \tau^-\tau^+$  processes, which include dipole moments of the  $\tau$  lepton, are implemented in the TauSpinner Monte Carlo program. A few examples of signatures of  $\tau\tau$  spin correlations and  $\tau$ -lepton dipole moments in observables are presented.

DOI:10.5506/APhysPolBSupp.19.2-A3

## 1. Introduction

Recent measurements of dipole moments of the  $\tau$  lepton at the Belle experiment [1], as well as observation of  $\gamma\gamma \rightarrow \tau^-\tau^+$  production at the LHC [2, 3], have brought considerable interest in magnetic and electric dipole moments of the  $\tau$  lepton. Deviation from predictions of the Standard Model (SM) and measured values can carry information on the New Physics (NP) effects, which are expected to be significantly enhanced for the  $\tau$  lepton compared to the muon. Various extensions of the SM, for example, new heavy particles in the loops, can be a source of NP contributions to dipole moments of the  $\tau$  lepton, as mentioned in [4, 5] and references therein.

---

\* Presented at the XLVI International Conference of Theoretical Physics “Matter to the Deepest”, Katowice, Poland, 15–19 September, 2025.

In our studies, the anomalous magnetic and electric dipole moments of the  $\tau$  lepton, or the corresponding form-factors in the case of a virtual photon and a  $Z$  boson, are introduced on top of simulations of  $\gamma\gamma \rightarrow \tau\tau$  and  $q\bar{q} \rightarrow \tau\tau$  processes in the SM including decays of the  $\tau$  leptons. The important ingredient in this calculation, which complicates consideration, is account of the spin correlations in the  $\tau$  pair. The Monte Carlo solutions are convenient and the calculations are implemented in the `TauSpinner` program [6, 7] for reweighting events with  $\tau$  leptons produced in the  $pp$  or PbPb collisions.

In the calculation of the hard quark–antiquark processes, the Improved Born Approximation (IBA) is applied, which includes electroweak (EW) corrections following the formalism outlined in Refs. [8, 9].

In this article, some aspects of the spin-correlation approach to the  $\gamma\gamma \rightarrow \tau\tau$  and  $q\bar{q} \rightarrow \tau\tau$  processes are reviewed. A few examples of the impact of the  $\tau$ -lepton dipole moments on observables in  $pp$  collisions are illustrated. Results presented here are based on Refs. [10–13].

## 2. Magnetic and electric dipole form-factors and moments

Magnetic and electric dipole moments of the  $\tau$  lepton induce its interaction with external magnetic,  $\vec{B}$ , and electric,  $\vec{E}$ , fields

$$H_{\text{int}} = -\vec{\mu}_\tau \vec{B} - \vec{d}_\tau \vec{E}, \quad (1)$$

where in the rest frame of the lepton, vectors of dipole moments are proportional to the  $\tau$ -lepton spin  $\vec{s}$

$$\vec{\mu}_\tau = g_\tau \frac{eQ_\tau}{2m_\tau} \vec{s}, \quad a_\tau = \frac{g_\tau}{2} - 1, \quad (2)$$

$$\vec{d}_\tau = \eta_\tau \frac{e}{2m_\tau} \vec{s}, \quad d_\tau = \frac{\eta_\tau}{2} \frac{e}{2m_\tau}. \quad (3)$$

Here,  $g_\tau$  is the  $g$ -factor,  $\eta_\tau$  is the dimensionless constant analogous to  $g_\tau$ ,  $a_\tau$  is the anomalous magnetic dipole moment, and  $d_\tau$  is the electric dipole moment in units  $e$  cm.

At high energies, one can use the Lorentz-covariant form of the  $\gamma\tau\tau$  vertex<sup>1</sup>

$$\Gamma_\gamma^\mu = -ieQ_\tau \left\{ F_1(q^2) \gamma^\mu + \frac{\sigma^{\mu\nu} q_\nu}{2m_\tau} [i F_2(q^2) + \gamma_5 F_3(q^2)] \right\} \quad (4)$$

in terms of the Dirac ( $F_1(q^2)$ ), Pauli ( $F_2(q^2)$ ), and electric dipole ( $F_3(q^2)$ ) form-factors, which reduce to the dipole moments at the real-photon point at  $q^2 = 0$

<sup>1</sup> The anapole form-factor  $F_A(q^2)$  is not considered here.

$$F_2(0) = a_\tau, \quad F_3(0) = \frac{2m_\tau}{eQ_\tau} d_\tau, \quad F_1(0) = 1. \quad (5)$$

In the following, we use the notation  $A(q^2) \equiv F_2(q^2)$  and  $B(q^2) \equiv F_3(q^2)$ .

At high energies of the LHC and future colliders, the  $Z$ -boson interaction with the  $\tau$  lepton (in general, with any fermion) becomes important, and the  $Z\tau\tau$  vertex including the SM contribution and dipole moment terms can be written as

$$\Gamma_Z^\mu = -i \frac{g_Z}{2} \left\{ \gamma^\mu (g_V^\tau - \gamma_5 g_A^\tau) + \frac{\sigma^{\mu\nu} q_\nu}{2m_\tau} [iX(q^2) + \gamma_5 Y(q^2)] \right\}. \quad (6)$$

Here,  $g_Z = e/(s_W c_W)$  is the constant of the neutral-current interaction,  $s_W \equiv \sin \theta_W$ ,  $c_W \equiv \cos \theta_W$ , where  $\theta_W$  is the weak mixing angle, and  $g_V^\tau$ ,  $g_A^\tau$  are the vector and axial-vector couplings.

In Eq. (6),  $X(q^2)$  is the weak anomalous magnetic form-factor (CP conserving), and  $Y(q^2)$  is the weak electric form-factor (CP violating), which on the  $Z$ -boson mass shell at  $q^2 = M_Z^2$  are related to the weak dipole moments as

$$X(M_Z^2) = a_\tau^{(w)} (2s_W c_W), \quad Y(M_Z^2) = d_\tau^{(w)} (2s_W c_W). \quad (7)$$

The weak dipole moments  $a_\tau^{(w)}$  and  $d_\tau^{(w)}$  are defined by the ALEPH Collaboration in Ref. [14].

In general, one has to separate the SM radiative corrections to the dipole moments, or form-factors, from NP contributions. For the real photons, the SM anomalous magnetic dipole moment was calculated in [5] with the result  $a_{\tau, \text{SM}} = 117721(5) \times 10^{-8}$ , and more recently in [15], where  $a_{\tau, \text{SM}} = (117717.1 \pm 3.9) \times 10^{-8}$ . For the finite  $q^2$ , one can use the QED contribution to  $A(q^2)$  in the first order in  $\alpha = e^2/(4\pi)$  [16].

The electric dipole moment is equal to  $d_{\tau, \text{SM}} = 7.32 \times 10^{-38} e \text{ cm}$ , which was calculated [17] in the SM including long-distance contributions. The SM prediction [18] for the weak anomalous magnetic moment is  $a_{\tau, \text{SM}}^{(w)} = -(2.10 + i 0.61) \times 10^{-6}$ .

In our calculation, we neglect minor contributions from the SM to the electric form-factor  $B(q^2)$ , as well as to the weak form-factors  $X(q^2)$  and  $Y(q^2)$ . These form-factors can be viewed as originating mainly from NP. As for the magnetic form-factor  $A(q^2)$ , the SM term is added via  $A(q^2) = A(q^2)_{\text{SM}} + A(q^2)_{\text{NP}}$ . To simplify further notation, we will not distinguish between form-factors and corresponding dipole moments for the NP contribution, and will denote them  $A_{\text{NP}}$ ,  $B_{\text{NP}} = B$ ,  $X_{\text{NP}} = X$ , and  $Y_{\text{NP}} = Y$ .

We should mention important relations between the NP contributions to these dipole moments and Wilson coefficients of the SM Effective Field Theory (SMEFT). The SMEFT Lagrangian is written as [19–21]

$$\mathcal{L}_{\text{SMEFT}} = \mathcal{L}_{\text{SM}}^{(4)} + \left( \frac{1}{\Lambda} \sum_k C_k^{(5)} Q_k^{(5)} + \frac{1}{\Lambda^2} \sum_k C_k^{(6)} Q_k^{(6)} + \mathcal{O}\left(\frac{1}{\Lambda^3}\right) + \text{H.c.} \right), \quad (8)$$

where  $\mathcal{L}_{\text{SM}}^{(4)}$  is the SM Lagrangian and  $\Lambda$  is the scale of NP.

Relevant for the dipole moments terms are the dimension-6 operators

$$Q_{\tau B}^{(6)} = (\bar{L}_L \sigma^{\mu\nu} \tau_R) \varphi B_{\mu\nu}, \quad Q_{\tau W}^{(6)} = (\bar{L}_L \sigma^{\mu\nu} \tau_R) \vec{\sigma} \varphi \vec{W}_{\mu\nu} \quad (9)$$

which enter Eq. (8) with the corresponding dimensionless Wilson coefficients  $C_{\tau B}^{(6)}$  and  $C_{\tau W}^{(6)}$ . In Eq. (9),  $\varphi$  is the scalar doublet,  $B_{\mu\nu}$  and  $\vec{W}_{\mu\nu}$  are the strength tensors for the  $U(1)_Y$  and  $SU(2)_L$  gauge fields  $B_\mu$  and  $\vec{W}_\mu$ ,  $\tau_R$  is the right-handed chiral spinor and  $\bar{L}_L = (\bar{\nu}_\tau \bar{\tau})_L$  contains the left-handed chiral adjoint spinors.

The straightforward calculation leads to the relations between the NP contributions to the dipole moments and Wilson coefficients

$$\begin{aligned} A_{\text{NP}} &= \lambda \text{Re}(D_{\gamma\tau\tau}), & B_{\text{NP}} &= -\lambda \text{Im}(D_{\gamma\tau\tau}), \\ X_{\text{NP}} &= \lambda \text{Re}(D_{Z\tau\tau}) (2s_W c_W), & Y_{\text{NP}} &= -\lambda \text{Im}(D_{Z\tau\tau}) (2s_W c_W), \end{aligned} \quad (10)$$

where

$$\lambda = \frac{\sqrt{2} v}{\Lambda^2} \frac{2m_\tau}{e}, \quad (11)$$

$$D_{\gamma\tau\tau} = c_W C_{\tau B}^{(6)} - s_W C_{\tau W}^{(6)}, \quad D_{Z\tau\tau} = s_W C_{\tau B}^{(6)} + c_W C_{\tau W}^{(6)} \quad (12)$$

and  $v = (\sqrt{2} G_F)^{-1/2} \approx 246$  GeV is the vacuum expectation value of the scalar field.

Once dipole moments are measured, the coefficients  $C_{\tau B}^{(6)}/\Lambda^2$  and  $C_{\tau W}^{(6)}/\Lambda^2$  can be determined which will indirectly constrain an underlying high-energy theory.

### 3. Spin correlations in the $\tau$ pair

Many details on inclusion of spins of the final  $\tau$  leptons in the  $e^- e^+ \rightarrow \tau^- \tau^+$ ,  $q\bar{q} \rightarrow \tau^- \tau^+$ , and  $\gamma\gamma \rightarrow \tau^- \tau^+$  processes are contained in Refs. [10, 12, 22]. Below, a few aspects of this approach are recalled.

The  $ab \rightarrow \tau^+ \tau^-$  process with  $(ab) = (e^- e^+)$ ,  $(q\bar{q})$  or  $(\gamma\gamma)$

$$a(k_1) + b(k_2) \rightarrow \tau^-(p_-) + \tau^+(p_+) \quad (13)$$

is described in the center-of-mass frame, where components of four-momenta are chosen as

$$\begin{aligned}
p_- &= (E, \vec{p}), & p_+ &= (E, -\vec{p}), & \vec{p} &= (0, 0, p), \\
k_1 &= (E, \vec{k}), & k_2 &= (E, -\vec{k}), & \vec{k} &= (E \sin \theta, 0, E \cos \theta),
\end{aligned} \quad (14)$$

so that  $\hat{3}$  axis is along vector  $\vec{p}$ , the reaction plane is spanned on  $\hat{1}$  and  $\hat{3}$  axes defined by the momenta  $\vec{p}$  and  $\vec{k}$ , and  $\hat{2}$  axis is along  $\vec{p} \times \vec{k}$ . Also,  $E = \frac{1}{2}\sqrt{s}$  is the energy,  $p = \beta E$  is the momentum, and  $\beta = (1 - 4\frac{m_\tau^2}{s})^{1/2}$  is the velocity of the  $\tau$  lepton.

After squaring the matrix element and averaging the result over the polarization states of the initial fermions or photons, one obtains

$$|\mathcal{M}|^2 = \sum_{i,j=1}^4 R_{ij} s_i^- s_j^+ = R_{44} \left( 1 + \sum_{i=1}^3 r_{i4} s_i^- + \sum_{j=1}^3 r_{4j} s_j^+ + \sum_{i,j=1}^3 r_{ij} s_i^- s_j^+ \right). \quad (15)$$

Here,  $\vec{s}^+ = (s_1^+, s_2^+, s_3^+)$  and  $\vec{s}^- = (s_1^-, s_2^-, s_3^-)$  are vectors of spins of the  $\tau^+$  and  $\tau^-$  leptons in their corresponding rest frames, and for convenience, we add the 4<sup>th</sup> components equal to 1, so that  $s_i^\pm \equiv (\vec{s}^\pm, 1)$  for  $i, j = 1, 2, 3, 4$ .

The elements of the spin-correlation matrix  $R_{ij}$  depend on the invariant mass of the  $\tau$  pair,  $m_{\tau\tau}$ , and the scattering angle  $\theta$ . In Eq. (15), the normalized elements of the matrix are introduced via  $r_{ij} \equiv R_{ij}/R_{44}$  ( $i, j = 1, 2, 3, 4$ ). The spin-independent element  $R_{44}$  determines the cross section for the unpolarized  $\tau$  leptons.

Elements  $R_{ij}$  were calculated in Refs. [10, 12, 22]. For the  $\gamma\gamma \rightarrow \tau\tau$  reaction, the tree-level  $t$ - and  $u$ -channel diagrams were taken into account including dipole moments up to the 4<sup>th</sup> order [12]. For the  $q\bar{q} \rightarrow \tau\tau$  processes, the  $s$ -channel exchange of virtual  $\gamma$  and  $Z$  boson was included, on top of which the EW corrections in the IBA were added [10, 13]. The contribution from the dipole form-factors was accounted for in the lowest order.

The elements  $(r_{14}, r_{24}, r_{34}) = \vec{\mathcal{P}}(\tau^-)$  and  $(r_{41}, r_{42}, r_{43}) = \vec{\mathcal{P}}(\tau^+)$  are components of polarization of the  $\tau^-$  and  $\tau^+$  leptons. These elements vanish for the  $\gamma\gamma \rightarrow \tau\tau$  reaction in a good approximation, while they are non-zero in the case of the  $q\bar{q} \rightarrow \tau\tau$  process. The elements  $r_{ij}$  with  $i, j = 1, 2, 3$  form a  $3 \times 3$  matrix of  $\tau^- \tau^+$  spin correlations.

Note that matrix  $R_{ij}$  has certain symmetry properties. In general, the following relations hold:

$$R_{ji} = R_{ij} \Big|_{A \rightarrow A, B \rightarrow -B, X \rightarrow X, Y \rightarrow -Y} \quad \text{for } i \neq j, \quad (16)$$

and some non-diagonal elements vanish if the dipole moments (form-factors) are switched off. In particular, if the electric dipole moment is absent, then for the  $\gamma\gamma \rightarrow \tau\tau$  process,  $R_{12} = R_{21} = R_{23} = R_{32} = 0$ .

#### 4. Results and discussion

In this section, a few numerical results for the  $\gamma\gamma \rightarrow \tau\tau$  and  $q\bar{q} \rightarrow \tau\tau$  processes are presented. We will discuss some observables, which can be studied in the experimental analyses.

Let us mention that the frame and sign convention of  $R_{ij}$  defined above differ from the ones used in the `TauSpinner` program, when the matrix is contracted with  $\tau$ -lepton polarimetric vectors. There are reasons for that frame orientation differences used in the `TauSpinner` and `TAUOLA` decay library [23], which are discussed in Ref. [12]. The result of the redefinition of the spin-correlation elements is

$$\begin{aligned}
 R_{tt} &= R_{44}, & R_{tx} &= -R_{42}, & R_{ty} &= -R_{41}, & R_{tz} &= -R_{43}, \\
 R_{xt} &= -R_{24}, & R_{xx} &= R_{22}, & R_{xy} &= R_{21}, & R_{xz} &= R_{23}, \\
 R_{yt} &= R_{14}, & R_{yx} &= -R_{12}, & R_{yy} &= -R_{11}, & R_{yz} &= -R_{13}, \\
 R_{zt} &= -R_{34}, & R_{zx} &= R_{32}, & R_{zy} &= R_{31}, & R_{zz} &= R_{33}. \quad (17)
 \end{aligned}$$

With this transformation,  $R_{ij}$  with  $i, j = t, x, y, z$  are used in the `TauSpinner` event reweighting algorithm for calculating weight implemented in the `TauSpinner` code and for presenting numerical results.

##### 4.1. Spin-correlation effects in $\gamma\gamma \rightarrow \tau\tau$ process

Results presented below are based on events generated with `PYTHIA 8.3` [24] using  $pp$  scattering at 13 TeV, `PhotonCollision:gmgm2tautau` hard process, parametrization of parton distribution functions `PDF:pSet = 13` and restricted to low invariant mass of the  $\tau$  pair,  $m_{\tau\tau} = 5\text{--}50$  GeV and transverse momentum  $p_{T}^{\tau\tau} > 5$  GeV. This choice of phase-space roughly corresponds to the range covered by the  $\text{PbPb} \rightarrow \text{Pb}(\gamma\gamma \rightarrow \tau\tau)\text{Pb}$  processes in peripheral PbPb collisions at the LHC.

The  $\tau$  decays were modeled with the `TAUOLA` decay library [23] (with no spin correlations between decaying  $\tau^+\tau^-$  leptons). In total there are about  $0.8 \times 10^6$  events for each decay mode generated. Then the spin correlations were added using weight calculated with `TauSpinner` program, both for the spin-correlation effects in the SM and in SM+NP models, and the cross-section normalization in SM+NP models.

We use as a reference the SM calculation with  $A = B = 0$ , and assume for simplicity that the QED radiative corrections are small enough and can be omitted when discussing the NP effects. Thus any non-zero values of  $A, B$  indicate some NP.

Below, the SM predictions are compared with the six settings for the dipole moments

$$\begin{aligned}
 (i) \quad & A = 0.002, 0.005, 0.02 \quad \text{with} \quad B = 0, \\
 (ii) \quad & B = 0.002, 0.005, 0.02 \quad \text{with} \quad A = 0.
 \end{aligned}
 \tag{18}$$

This choice is arbitrary covering the plausible range. The smallest value  $A = 0.002$  roughly corresponds to  $2a_{\tau, \text{SM}}$ .

The analysis shows that the behavior of the matrix  $r_{ij}$  is not trivial. In some cases, its elements are zero in the SM, while they obtain contribution from the dipole moments. In many cases, the spin correlations in the SM are sizable and dominate over the impact from the dipole moments. This can give hints on how to optimize the choice of the observables and minimize background, and at the same time, underlying importance of spin correlations as a possible bias for the cross sections.

Let us discuss distributions constructed from momenta of the  $\tau$ -decay products. The following example of the decay channels  $\tau^- \rightarrow \rho^- \nu_\tau \rightarrow \pi^- \pi^0 \nu_\tau$  and  $\tau^+ \rightarrow \rho^+ \bar{\nu}_\tau \rightarrow \pi^+ \pi^0 \bar{\nu}_\tau$  is considered.

In Fig. 1, the effect of spin correlations in the SM with  $A = B = 0$  is shown on a few distributions:

- (i) transverse momenta of charged pions  $p_T^\pi$ ,
- (ii) ratios  $E_\rho/E_\tau$  and  $E_{\pi^\pm}/E_\rho$ ,
- (iii) ratio of invariant mass of  $\rho^+ \rho^-$  system to  $\tau^+ \tau^-$  system,  $m_{\rho\rho}/m_{\tau\tau}$ .

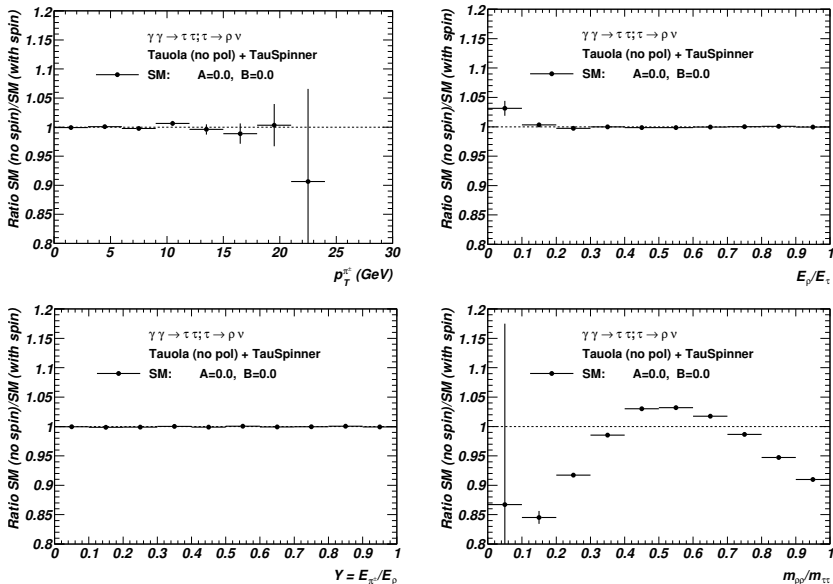


Fig. 1. Spin-correlation effects in  $\gamma\gamma \rightarrow \tau\tau$  for  $\tau$ -decay channels:  $\tau^- \rightarrow \rho^- \nu_\tau \rightarrow \pi^- \pi^0 \nu_\tau$  and  $\tau^+ \rightarrow \rho^+ \bar{\nu}_\tau \rightarrow \pi^+ \pi^0 \bar{\nu}_\tau$ . The ratio (SM without spin correlations)/(SM with spin correlations) is shown. The figure is taken from Ref. [12].

The  $p_T^\pi$ ,  $E_\rho/E_\tau$ , and  $E_{\pi^\pm}/E_\rho$  distributions are insensitive to the spin correlations. However, in the distribution of  $m_{\rho\rho}/m_{\tau\tau}$ , the effect is apparent. The change in the shape of the latter is 10–15% in a wide range around  $m_{\rho\rho}/m_{\tau\tau} \approx 0.5$ .

Fig. 2 shows the effect of SM+NP including non-zero dipole moments and spin correlations. Once integrated over the full phase-space, the impact from SM+NP extension is mostly due to the change of the cross section. Still changes in the shape of the  $p_T^\pi$  distribution are observed, with the ratio (SM+NP)/SM increasing with increasing  $p_T^\pi$ . Some effects are also visible in the  $E_\rho/E_\tau$ ,  $E_{\pi^\pm}/E_\rho$ , and  $m_{\rho\rho}/m_{\tau\tau}$  distributions for  $A = 0.02$ . However, without detector studies, it is not clear how useful these effects can be for measurements searching for effects of NP.

#### 4.2. Spin-correlation effects in $q\bar{q} \rightarrow \tau\tau$ process

Results for the  $q\bar{q} \rightarrow \tau\tau$  process are also based on the events generated by PYTHIA 8.3 [24] for the  $pp$  collisions at 13 TeV, and the  $\tau\tau$  invariant-mass range  $m_{\tau\tau} = 65$ –150 GeV. The  $\tau$  decays  $\tau^\pm \rightarrow \rho^\pm \nu_\tau$  are modeled with the TAUOLA decay library [23], and correlations were added using the weight calculated with the TauSpinner program.

In the chosen region of  $\tau\tau$  invariant mass close to the  $Z$ -boson peak, there is practically no dependence on the form-factors  $A(q^2)$  and  $B(q^2)$ , however, this region can be suitable for searching for signatures of the weak form-factors  $X(q^2)$  and  $Y(q^2)$ .

The polarization and spin-correlation effects are illustrated for a few variables calculated from the momenta of  $\tau$ -decay products:

- (i) ratios  $E_\rho/E_\tau$  and  $E_{\pi^\pm}/E_\rho$ , which are sensitive to longitudinal polarization,
- (ii) ratio of invariant masses of  $\rho^+\rho^-$  system and  $\tau^+\tau^-$  system,  $m_{\rho\rho}/m_{\tau\tau}$ , which is sensitive to longitudinal spin correlations,
- (iii) two acoplanarity angles  $\Psi$  and  $\phi^*$ , which are sensitive to transverse–transverse and transverse–normal spin correlations.

The definition of the  $\Psi$  angle is chosen following the LEP publications [25, 26]. The direction of the initial quark (beam) is assumed to be along the  $z$ -axis in the laboratory frame. The four-momenta of  $\tau$ -decay products and beam momentum are boosted to the rest frame of the  $\rho^+\rho^-$  system. In this system, the vectors of momenta are rotated around  $z$ - and  $y$ -axes such that  $\pi^-$  is along the  $z$ -axis, and  $\pi^+$  lies in the  $xz$ -plane. Then  $\Psi$  is the angle between the beam direction and  $\pi^-$  direction.

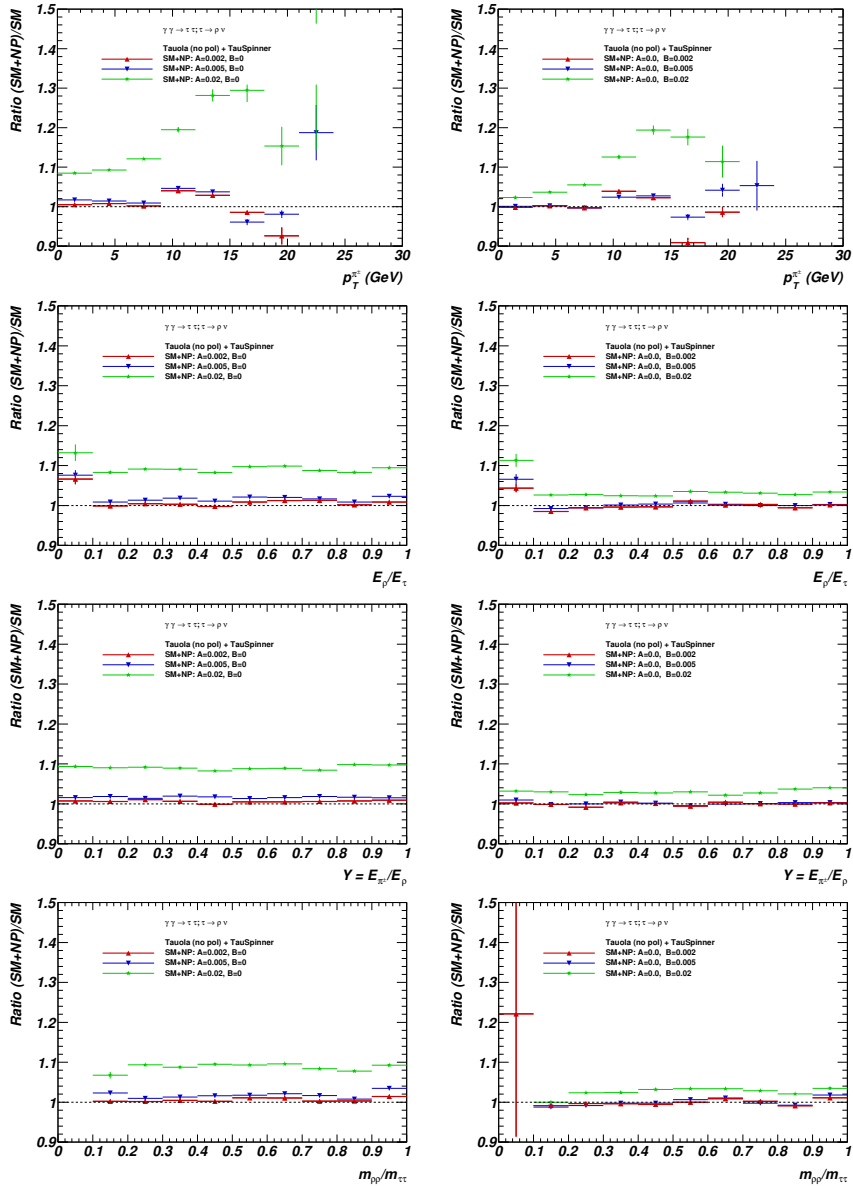


Fig. 2. Kinematical distributions in the  $\gamma\gamma \rightarrow \tau\tau$  process for  $\tau$ -lepton decays  $\tau^\pm \rightarrow \rho^\pm \nu_\tau \rightarrow \pi^\pm \pi^0 \nu_\tau$ . Compared are the calculations in SM and SM+NP with the sets:  $A = 0.002, 0.005, 0.02, B = 0$  (left column) and  $A = 0.0, B = 0.002, 0.005, 0.02$  (right column). The figure is taken from Ref. [12].

The  $\phi^*$  angle was proposed for the Higgs CP studies in [27] and was used in the measurements at the LHC [28, 29]. It is the angle between the planes spanned on  $\pi^\pm, \pi^0$  momenta for each  $\tau^\pm$  decay, calculated in the rest frame of the  $\rho^+\rho^-$  system. In this case, to preserve sensitivity to the transverse spin correlations, the sample has to be split depending on the angle  $\alpha_\rho$  between the beam axis and the plane spanned over  $\pi^\pm, \pi^0$  from one decaying  $\tau$  lepton, calculated in the laboratory frame (splitting into regions:  $\alpha_\rho < \pi/4$  and  $\alpha_\rho > \pi/4$ ).

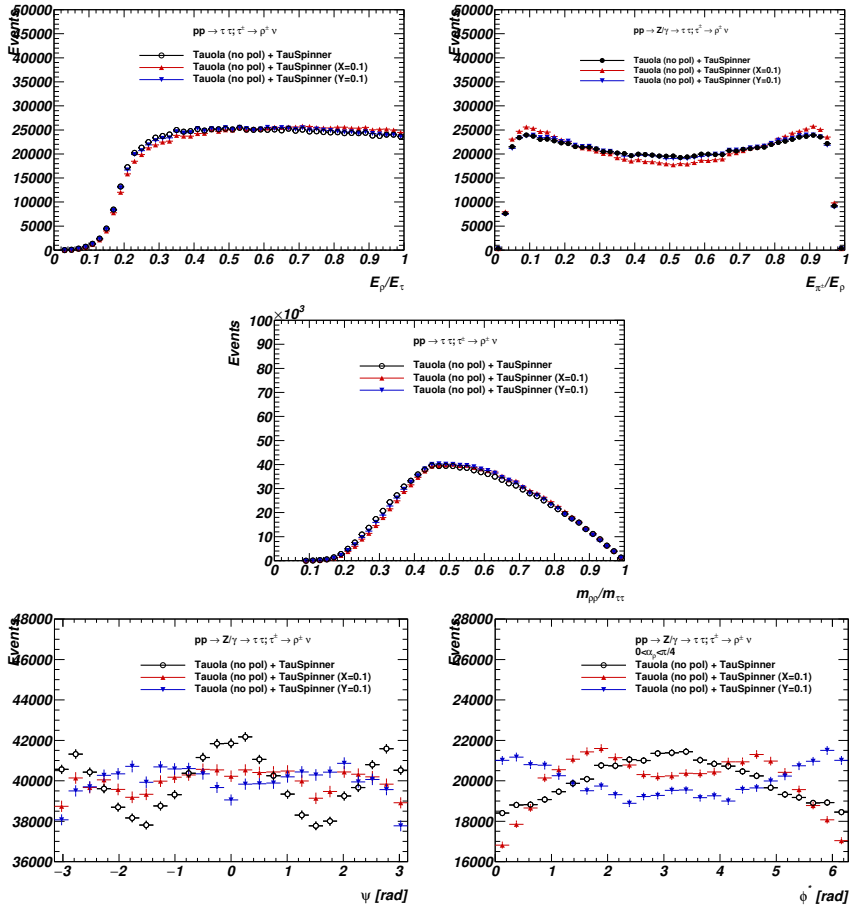


Fig. 3. Distribution of several observables (see the text) for the  $q\bar{q} \rightarrow \tau\tau$  process. Compared are the SM predictions (black open circles) for  $X = Y = 0$  and the NP ones (red and blue triangles) for  $X = 0.1$  or  $Y = 0.1$ . Both  $\tau$  leptons decay into the  $\tau^\pm \rightarrow \rho^\pm \nu_\tau \rightarrow \pi^\pm \pi^0 \nu_\tau$  channels. The figure is taken from Ref. [13].

Distribution of spin-correlation sensitive observables in the SM with  $X = Y = 0$  and in the NP models with non-zero weak dipole moments is shown in Fig. 3. Distributions of  $E_\rho/E_\tau$ ,  $E_{\pi^\pm}/E_\rho$ , and  $m_{\rho\rho}/m_{\tau\tau}$  show some effect of changed component  $r_{tz}$  for  $X = 0.1$ .

Both  $\Psi$  and  $\phi^*$  distributions have a cosine-like shape, once the sample is split into the two sub-samples depending on the sign of the product  $y_{\tau^+} \cdot y_{\tau^-}$ , where  $y_{\tau^\pm} = (E_{\pi^\pm} - E_{\pi^0})/(E_{\pi^\pm} + E_{\pi^0})$ . If  $y_{\tau^+} \cdot y_{\tau^-} < 0$ , the angles are shifted as follows:  $\Psi \rightarrow \Psi - \pi/2$  and  $\phi^* \rightarrow \phi^* - \pi$ . This shift is included into definition of  $\Psi$  and  $\phi^*$ , and then the final adjustment is made to respect periodicity for  $-\pi \leq \Psi \leq \pi$  and  $0 \leq \phi^* \leq 2\pi$ . The periodical characteristic of the  $\Psi$  and  $\phi^*$  distributions arise due to non-zero components  $r_{xx}$ ,  $r_{yy}$  of the spin-correlation matrix. At the same time the phase of the distributions is sensitive to non-diagonal components  $r_{yx}$ ,  $r_{xy}$ .

The dipole moments influence  $\Psi$  and  $\phi^*$  distributions either by flattening the cosine-like pattern in the  $\Psi$  distribution, or by changing the phase in the  $\phi^*$  distribution. These effects are due to the changes in  $r_{yy}$  for  $X = 0.1$ , and in  $r_{xy}$  for  $Y = 0.1$ . However, the interplay between changes in the spin-correlation elements and distributions of acoplanarity angles seems nontrivial.

## 5. Summary

In this article, the approach to implementing effects of electromagnetic and weak dipole moments (form-factors) in the  $\gamma\gamma \rightarrow \tau\tau$  and  $q\bar{q} \rightarrow \tau\tau$  processes is reviewed. This topic is relevant in view of the experiments on the  $\tau$ -pair production in  $pp$  and PbPb collisions at the LHC. The approach is based on the inclusion of spins of the final  $\tau$  leptons in the parton-level  $2 \rightarrow 2$  processes.

The components of spin-correlation matrices in  $pp \rightarrow \tau\tau$  production with subsequent  $\tau$  decays are studied in order to determine which of them are sensitive to the dipole moments, and can be useful for constructing kinematical observables.

Several semi-realistic observables were studied, in particular, those built on momenta of the pions from the  $\tau$ -lepton decays  $\tau^+ \rightarrow \rho^+ \bar{\nu}_\tau \rightarrow \pi^+ \pi^0 \bar{\nu}_\tau$ ,  $\tau^- \rightarrow \rho^- \nu_\tau \rightarrow \pi^- \pi^0 \nu_\tau$ . These decay channels of the  $\tau$  lepton are selected due to sensitivity to the transverse components of the spin-correlation matrix. The consideration is focused on the transverse spin correlations as they are not often discussed in the literature, in particular, in  $pp$  collisions.

This analysis is performed for the  $\gamma\gamma \rightarrow \tau\tau$  and  $q\bar{q} \rightarrow \tau\tau$  parton processes in the  $pp$  collisions at the LHC energies. In the  $q\bar{q} \rightarrow \tau\tau$  process near the  $Z$ -boson peak, the dipole moments are included on top of the Standard Model amplitudes supplemented with electroweak corrections in the framework of the Improved Born Approximation. These ingredients were installed into the TauSpinner event reweighting algorithm.

It is shown that exploring spin effects in the final  $\tau$  pair can enhance the sensitivity of some observables in high-energy experiments to New Physics signatures, in particular, to the anomalous magnetic and electric dipole moments (form-factors) of the  $\tau$  lepton.

The author would like to thank the organizers of the Conference “Matter to the Deepest” 2025 in Katowice, Poland for the invitation to present the talk and hospitality. The author is grateful to Elzbieta Richter-Was and Zbigniew Was for fruitful collaboration on the topics discussed in this talk. This project was supported in part by funds of the National Science Centre (NCN), Poland, grant No. 2023/50/A/ST2/00224 and of the COPIN-IN2P3 Collaboration with LAPP-Annecy, France.

## REFERENCES

- [1] Belle Collaboration (K. Inami *et al.*), *J. High Energy Phys.* **2022**, 110 (2022), [arXiv:2108.11543 \[hep-ex\]](#).
- [2] ATLAS Collaboration (G. Aad *et al.*), *Phys. Rev. Lett.* **131**, 151802 (2023), [arXiv:2204.13478 \[hep-ex\]](#).
- [3] CMS Collaboration (A. Tumasyan *et al.*), *Phys. Rev. Lett.* **131**, 151803 (2023), [arXiv:2206.05192 \[nucl-ex\]](#).
- [4] W. Bernreuther, A. Brandenburg, P. Overmann, *Phys. Lett. B* **39**, 1413 (1997); *Erratum ibid.* **412**, 425 (1997).
- [5] S. Eidelman, M. Passera, *Mod. Phys. Lett. A* **22**, 159 (2007), [arXiv:hep-ph/0701260](#).
- [6] Z. Czyzula, T. Przedzinski, Z. Was, *Eur. Phys. J. C* **72**, 1988 (2012), [arXiv:1201.0117 \[hep-ph\]](#).
- [7] T. Przedzinski, E. Richter-Was, Z. Was, *Eur. Phys. J. C* **79**, 91 (2019), [arXiv:1802.05459 \[hep-ph\]](#).
- [8] D.Yu. Bardin *et al.*, *Comput. Phys. Commun.* **133**, 229 (2001), [arXiv:hep-ph/9908433](#).
- [9] E. Richter-Was, Z. Was, *Eur. Phys. J. C* **79**, 480 (2019), [arXiv:1808.08616 \[hep-ph\]](#).
- [10] S. Banerjee, A.Y. Korchin, E. Richter-Was, Z. Was, *Phys. Rev. D* **109**, 013002 (2024), [arXiv:2307.03526 \[hep-ph\]](#).
- [11] A.Y. Korchin, *Acta Phys. Pol. B Proc. Suppl.* **17**, 5-A20 (2024).
- [12] A.Y. Korchin, E. Richter-Was, Z. Was, *Acta Phys. Pol. B* **56**, 10-A4 (2025), [arXiv:2506.15213 \[hep-ph\]](#).
- [13] A.Y. Korchin, E. Richter-Was, Z. Was, [arXiv:2512.22971 \[hep-ph\]](#).
- [14] ALEPH Collaboration (A. Heister *et al.*), *Eur. Phys. J. C* **30**, 291 (2003), [arXiv:hep-ex/0209066](#).

- [15] A. Keshavarzi, D. Nomura, T. Teubner, *Phys. Rev. D* **101**, 014029 (2020), [arXiv:1911.00367 \[hep-ph\]](#).
- [16] V.B. Berestetskii, E.M. Lifshitz, L.P. Pitaevskii, «Quantum Electrodynamics, Volume 4 Course of Theoretical Physics», Pergamon Press, Oxford 1982.
- [17] Y. Yamaguchi, N. Yamanaka, *Phys. Rev. D* **103**, 013001 (2021), [arXiv:2006.00281 \[hep-ph\]](#).
- [18] J. Bernabéu, G.A. González-Sprinberg, M. Tung, J. Vidal, *Nucl. Phys. B* **436**, 474 (1995), [arXiv:hep-ph/9411289](#).
- [19] W. Buchmüller, D. Wyler, *Nucl. Phys. B* **268**, 621 (1986).
- [20] J.A. Aguilar-Saavedra, *Nucl. Phys. B* **812**, 181 (2009), [arXiv:0811.3842 \[hep-ph\]](#).
- [21] B. Grzadkowski, M. Iskrzyński, M. Misiak, J. Rosiek, *J. High Energy Phys.* **2010**, 085 (2010), [arXiv:1008.4884 \[hep-ph\]](#).
- [22] S. Banerjee, A.Y. Korchin, Z. Was, *Phys. Rev. D* **106**, 113010 (2022), [arXiv:2209.06047 \[hep-ph\]](#).
- [23] S. Jadach, Z. Wąs, R. Decker, J.H. Kühn, *Comput. Phys. Commun.* **76**, 361 (1993).
- [24] C. Bierlich *et al.*, *SciPost Phys. Codebases* **8**, 1 (2022), [arXiv:2203.11601 \[hep-ph\]](#).
- [25] ALEPH Collaboration (R. Barate *et al.*), *Phys. Lett. B* **405**, 191 (1997).
- [26] DELPHI Collaboration (P. Abreu *et al.*), *Phys. Lett. B* **404**, 194 (1997).
- [27] K. Desch, A. Imhof, Z. Wąs, M. Worek, *Phys. Lett. B* **579**, 157 (2004), [arXiv:hep-ph/0307331](#).
- [28] ATLAS Collaboration (G. Aad *et al.*), *Eur. Phys. J. C* **83**, 563 (2023), [arXiv:2212.05833 \[hep-ex\]](#).
- [29] CMS Collaboration (A. Tumasyan *et al.*), *J. High Energy Phys.* **2022**, 012 (2022), [arXiv:2110.04836 \[hep-ex\]](#).